Quantum Mechanical and Kinetic Studies of the Reaction of Methyl Radicals with Chlorine Molecules

Evangelos Drougas, Demetrios K. Papayannis, and Agnie M. Kosmas*

Department of Chemistry, University of Ioannina, Greece 45110

Received: August 8, 2001; In Final Form: April 19, 2002

Quantum mechanical electronic structure calculations were carried out to determine equilibrium geometries, energetics, and normal-mode frequencies for stationary points along the minimum energy reaction path for the reaction of methyl radicals with chlorine molecules. The results are used to calculate the rate coefficient, employing both extended RRKM theory and quasi-classical trajectory techniques. The results of both methods agree well with each other and with the experimental measurements. The reactivity is investigated and is shown to be greatly enhanced by increasing the initial translational energy of the reactants. A large part of the total available energy is shown to be directed into product vibration, in good consistency with the experimental observations.

1. Introduction

The reactions between hydrocarbon free radicals (R) and chlorine molecules are important elementary steps in both thermal and photochemical chlorination processes[1] which take place via the simple two-step free-radical chains:

$$RH + Cl \rightarrow HCl + R \qquad (1)$$

$$R + Cl_2 \rightarrow RCl + Cl \qquad (2)$$

Of these, Cl atom reactions have been widely investigated partly due to their importance in atmospheric processes[2] and also because fundamental information on energy disposal in exoergic chemical reactions can be obtained from a detailed analysis of the infrared emission of HCl, usually produced with a significant amount of vibrational and rotational excitation.[3] Studies of the reactions of alkyl and substituted alkyl radicals with Cl_2 and other halogen molecules are much less frequent in the literature and theoretical investigations of the kinetics and dynamics of such systems are yet more scarce. Another point that makes interesting the study of such systems is the ambiguous conception postulated in the literature that several reactions of alkyl and substituted alkyl radicals with halogen molecules possess negative activation energies.[4−6]

Recent experimental studies of reaction 2 with R being the methyl radical include a molecular beam dynamical investigation[7] and measurements of the rate coefficient at various temperatures.[8−11] Values at room temperature were found to range from $(1.5 \pm 0.1) \times 10^{-12}$ to $(3.4 \pm 0.3) \times 10^{-12}$ cm³ molecule⁻¹ s⁻¹. Kovalenko and Leone[12] in a detailed treatment of their experimental measurements have shown that the increase in initial translational energy yields a considerable enhancement in the reactivity of the $CH_3 + Cl_2$ system. Also they have found that a large amount of total available energy is directed into product vibration. Timonen et al.[5,8−10] have studied the kinetics of several alkyl radical reactions with dihalogens over the temperature range 296 to 712 K and concluded that the $CH_3 + Cl_2$ reaction, contrary to other alkyl + Cl_2 systems, presents a

small positive activation energy which is in accord with the translational energy enhancement observed. Very recently Dobis and Benson[11] have measured again the rate coefficient and have established the positive activation energy of reaction 2 for R = CH_3 and C_2H_5. In their critical examination of several data for various R + Cl_2 reactions[13] they dispute the concept of negative activation energies for some members of this class of reactions and they conclude that the apparent negative activation energies observed in some cases must be artifacts of the experimental techniques employed.

The few theoretical investigations include mainly the examination of the transition states of a series of alkyl and chloroalkyl radical reactions with Cl_2[14,15] and a recent study of the stationary points in the reactions of methyl and ethyl radicals with Cl_2 by Bozzelli and co-workers.[16] In all these studies a transition state was determined at the entrance of the reaction, possessing a linear geometry in the three atomic centers involved, i.e., C, Cl, and Cl′.

In the present work we reexamine the various stationary points of the $CH_3 + Cl_2$ reaction at a higher level of theory. Using these findings theoretical rate constants were calculated on the basis of an extension of RRKM theory and on quasi-classical trajectory techniques, using a LEPS-type potential energy surface fitted to the ab initio results for the stationary points. This latter method allowes us to investigate at a first approximation the question of initial collision energy dependence and the disposal of total available energy, to compare with the experimental investigation of Kovalenko and Leone.[12]

2. Quantum Mechanical Calculations and Results

The geometries of reactants, products, transition states, and intermediate complexes have been fully optimized at the MP2-(full)/ 6-311+G(3df, 3dp) level of theory, starting from the C_1 geometry. Vibrational frequencies were calculated at the same level and were used for the characterization of the stationary points and the calculation of the zero-point-energy (ZPE) corrections. The stationary points have been positively identified as minima (number of imaginary frequencies NIMAG = 0) or transition states (NIMAG = 1). Connection of the transition
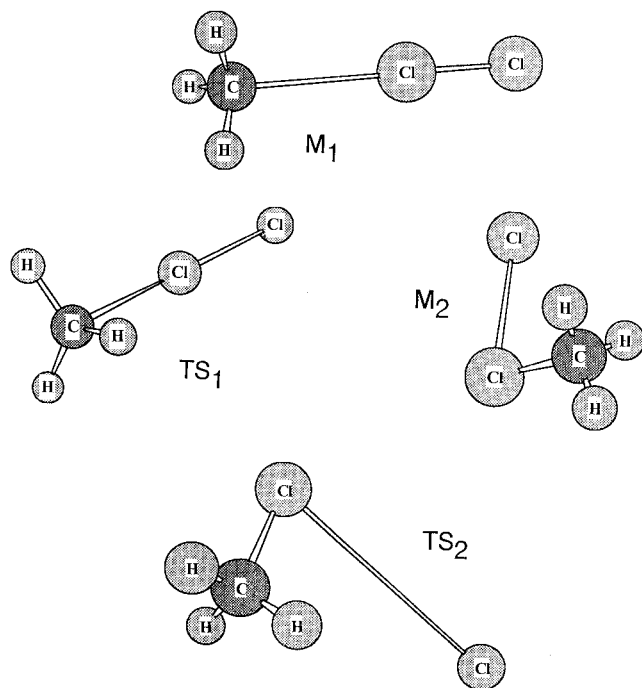

Figure 1. Structures of stationary points for the reaction $CH_3 + Cl_2$.

TABLE 1: Optimized Geometries in Å and deg for Reactants, Products, Transition States, and Reaction Intermediates[a]

	M_1	M_2	TS_1	TS_2	CH_3	Cl_2	CH_3Cl
$r(CCl)$	2.8733	1.7677	2.2653	1.7916			1.7652
	3.0975	1.7786	2.3302				
$r(ClCl')$	1.9918	2.8256	2.0541	4.3000		1.9796	
	2.0350	3.3008	2.0979				
$r(CH)$	1.0740	1.0841	1.0759	1.0841	1.0735		1.0826
	1.0797	1.0879	1.0818				
$r(CH')$	1.0740	1.0836	1.0759	1.0837			1.0826
$\angle CClCl'$	180.0	89.7	180.0	89.8			
	180.0	89.1	180.0				
$\angle HCCl$	92.1	108.1	98.2	108.4			108.7
	93.7	108.7	98.1				
$\angle HCH'$	120.0	110.8	118.0	110.5	120.0		110.2
	119.9	110.2	118.0				
$\varphi(HCClCl')$	0.0	180.0	0.0	162.1			
$\varphi(H'CClCl')$	120.0	59.9	120.0	39.6			

[a] The second line contains results of ref 16 at the MP2/ 6-311G(d, p) level of theory.

state with reactants and products has been confirmed by intrinsic reaction coordinate (IRC)[17] calculations. The moments of inertia and the partition functions determined were used for the RRKM calculations of the rate coefficient. Finally, single-point CCSD-(T)/ 6-311+G(3df, 3dp) calculations at the MP2(full)/ 6-311+G-(3df, 3dp) geometries were carried out to establish a higher accuracy for the energetics. The calculations were performed using the GAUSSIAN 98 series of programs[18] on a Silicon Graphics Origin 2000/10 R10000 at the University of Ioannina, Greece.

Three stationary points were determined along the reaction path, two of them representing energy minima and one corresponding to a well-defined tight transition state. All structures are depicted in Figure 1 and their properties along with those of reactants and products are summarized in Tables 1, 2 and 3 where they are compared with the corresponding results of Bozzelli and co-workers.[16] As it is readily seen, our calculated
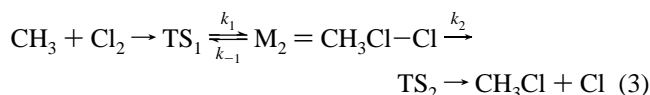
bond equilibrium distances at the MP2(full)/ 6-311G+(3df, 3dp) are shorter than the corresponding values of ref 16 calculated at the MP2/6-311G(d, p) level. However, the same general characteristics for the reaction path are confirmed. As the reactants CH_3 and Cl_2 approach, they form a loose, shallow van der Waals structure, CH_3-Cl_2, denoted hereafter as M_1, at the entrance of the potential energy surface and located at a C−Cl distance of 2.87 Å, 0.85 kcal mol^{-1} below the reactants at the CCSD(T) level. This adduct with a linear C−Cl−Cl geometry proceeds to a well-defined tight transition state, TS_1, with an imaginary frequency 383i and with a similar linear C−Cl−Cl geometry but with the C−Cl distance decreased significantly from 2.87 in M_1 to 2.26 Å in TS_1 while the Cl−Cl distance is increased from 1.99 to 2.05 Å. Similar linear-type configurations of TS_1 have been identified by both Tirtowidjojo[14] and Seetula[15] in a series of alkyl and chloroalkyl radicals with Cl_2. Also, similar behavior has been determined in the ab initio investigation of the analogous H + Cl_2 system where the two angular transition states identified present really negligible or very small barriers to linearity.[19]

The calculated energy barrier values corresponding to TS_1 are rather confused. Our MP2(full)/ 6-311+G(3df, 3dp) calculations locate TS_1 below the reactants but the CCSD(T) calculations including ZPE corrections place clearly TS_1 at 1.24 kcal mol^{-1} above reactants. In the work of Bozzelli and co-workers[16] the MP2 calculations locate TS_1 at 2.4 kcal mol^{-1} above reactants and the CBSQ// MP2/6-311G(d, p) calculations below. We attribute this difference with our energetic results to the significant deviations existing in the optimized geometries of Bozzelli's and ours, which affect the single-point calculations at a higher level of theory.

The system further proceeds to a minimum M_2 of the form CH_3Cl-Cl with a H^{1}C−ClCl' trans geometry, located at a considerable potential well, 32.44 kcal mol^{-1}, with respect to reactants. The carbon−chlorine bond is almost completed and the second chlorine atom begins to move away. M_2 decomposes into the products CH_3Cl + Cl that are formed at an energy barrier of 2.23 kcal mol^{-1} above the M_2 well and 30.2 kcal mol^{-1} below the reactants including zero-point energy corrections. This result is in reasonable agreement with the experimental exothermicity used by Timonen and Gutman,[8] 108 kJ mol^{-1}. The course of the reaction as described above, presents similar characteristics with the systems $CH_3 + H_2$,[20,21] and CH_3 + Br_2, I_2,[7,12,22,40] and indicates a similar pattern for the CH_3 + X_2 (X = H, halogen atom) reactions with dynamics largely governed by long-range attractive forces.

3. RRKM Calculations and Results

In this section we apply extended RRKM theory for the calculation of the macrocanonical bimolecular rate constant, $k(T)$,[23−25] assuming the following general scheme

$$CH_3 + Cl_2 \rightarrow TS_1 \underset{k_{-1}}{\overset{k_1}{\rightleftharpoons}} M_2 = CH_3Cl-Cl \overset{k_2}{\rightarrow}$$
$$TS_2 \rightarrow CH_3Cl + Cl \quad (3)$$

where k_1 and k_2 are the microcanonical forward rate constants and k_{-1} the corresponding backward. The M_1 = CH_3-Cl_2 adduct is not included since it is found too shallow, −0.85 kcal mol^{-1} at the CCSD(T) level, to play any significant role in the calculation of the rate coefficient. For this reason it is ignored in the above formulation. The two reactants are assumed to follow a potential energy profile such as given in Figure 2, where the reaction proceeds through the tight transition state TS_1 to

Reaction of Methyl Radicals with Chlorine Molecules

J. Phys. Chem. A, Vol. 106, No. 26, 2002 **6341**

TABLE 2: Electronic Energies in h and Relative Energetics Including ZPE Corrections in kcal mol^{-1}, for the CH$_3$ + Cl$_2$ Reaction[a]

species	MP2(full)/ 6-311+G(3df, 3dp)[b]		CBSQ// MP2/ 6-311G(d,p)[c]		CCSD(T)// MP2/ 6-311+G(3df, 3dp)[b]		ZPE
CH$_3$ + Cl$_2$	−959.30592	0.00	−959.19724	0.00	−959.37978	0.00	19.69
M$_1$	−959.31092	−2.01	−959.19954	−1.45	−959.38292	−0.85	20.81
TS$_1$	−959.31543	−3.65	−959.20158	−2.72	−959.38147	1.24	21.99
M$_2$	−959.36685	−32.56	−959.24236	−34.82	−959.43927	−32.44	24.55
TS2	−959.35901	−28.97			−959.43492	−30.19	24.07
CH$_3$Cl + Cl	−959.36030	−28.99	−959.23865	−32.49	−959.43621	−30.21	24.86

[a] The results of each method contain the total electronic energies and the energy differences with respect to reactants, including zero-point energy corrections. [b] Results of present work. [c] Results of ref 16.

TABLE 3: Moments of Inertia (amu Å^2) and Harmonic Frequencies (cm^{-1}) for Stationary Points of Reaction CH$_3$ + Cl$_2$

species	I_a,	I_b,	I_c	frequencies					
M$_1$	3.48	256.61	256.61	3360, 565,	3360, 188,	3160, 188,	1441, 108,	1441, 69,	602, 69
TS$_1$	3.45	220.03	220.03	3332, 533,	3332, 533,	3143, 448,	1424, 91,	1424, 91,	960, 383i
M$_2$	36.81	190.57	224.19	3262, 1054,	3258, 1050,	3143, 771,	1491, 110,	1489, 91,	1396, 59
TS$_2$	3.15	24.5	245.35	3218, 1049,	3216, 1049,	3105, 750,	1496, 51,	1495, 13,	1394, 34i
CH$_3$	1.73,	1.73,	3.46	3363,	3363,	3164,	1443,	1443,	503
Cl$_2$	0.0,	71.79,	71.79	562					
CH$_3$Cl	3.19,	38.24,	38.24	3216, 1050,	3216, 750	3104,	1499,	1394,	1050,
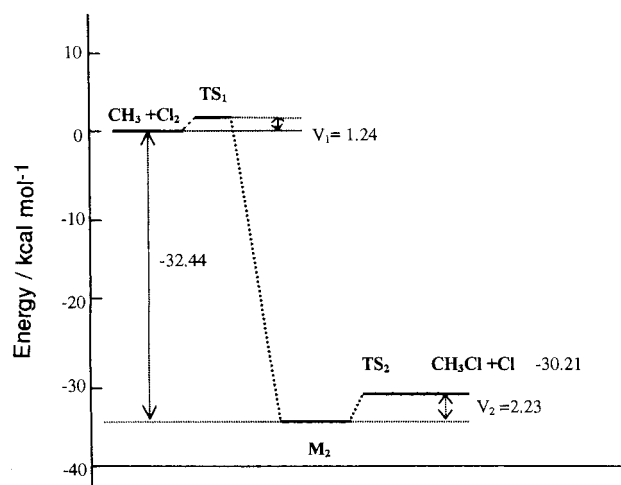
Figure 2. Schematic representation of the reaction profile. Numbers indicate energy differences in kcal mol^{-1}.

the potential well M$_2$ = CH$_3$Cl−Cl. The intermediate complex M$_2$ is formed "hot" in the low-pressure limit and its formation is hindered by the potential barrier V_1 with respect to reactants, corresponding to TS$_1$. Generally, a transition state TS$_2$ also hinders the decomposition of the intermediate activated complex M$_2$ to products with a corresponding potential barrier V_2 which may be positive or negative with respect to reactants but greater than the potential well V_{M_2} corresponding to M$_2$. Therefore, the reaction is analyzed from the point of view of the options available to the intermediate minimum M$_2$ and the overall reaction rate coefficient, $k(T)$, will include the rate constant for each step.

The microcanonical rate constant, $k_i(E)$, at an energy E, for each elementary step in reaction 3 is given by[26,27]

$$k_i(E, J) = W_i(E, J)/h\rho_{reag}(E, J) \qquad (4)$$

where $W_i(E, J)$ is the number of states for the active degrees of

freedom of the transition state TS$_i$ being involved in the considered reaction step i, and $\rho_{reag}(E, J)$ is the density of states for the active degrees of freedom available to the reacting species.

The macrocanonical rate constant for the overall reaction is then given as

$$k(T) = \frac{1}{hQ_{CH_3}Q_{Cl_2}} \sum_{J=0}^{\infty} \int_{V_{max}}^{\infty} \frac{W_2(E, J)e^{-E/RT}}{1 + \beta(E, J)} dE \qquad (5)$$

where $\beta(E, J)$ is the microcanonical branching ratio

$$\beta(E, J) = k_2(E, J)/k_{-1}(E, J) = W_2(E, J)/W_{-1}(E, J) \qquad (6)$$

and Q_{CH_3}, Q_{Cl_2} the corresponding partition functions. The quantity $W_2(E, J)$ and the microcanonical rate constants $k_2(E, J)$ and $k_{-1}(E, J)$ are evaluated using a modified version of the RRKM code[28] based on RRKM theory.[26,27] The symmetry number required in the input of the RRKM algorithm, i.e., the symmetry of the internal rotor of the critical configuration and the energy minimum,[28] is also taken from the Gaussian output and it has the value 3. The rate coefficient, $k(T)$, is finally evaluated by direct summation and numerical integration of eq 5, with V_{max} being the greater of V_1 or V_2.

In the present case a tight transition state TS$_2$ that generally hinders the decomposition of the minimum into products has not been determined, i.e., the minimum follows a barrierless dissociation pathway. Hence, to determine the critical configuration in the exit valley, where the number of states is a minimum, a variational treatment [29−31] was employed, i.e., a number of energy points at the exit path have been calculated by increasing the Cl−Cl distance and rate constant computations have been carried out at these points. The location where the rate coefficient assumes a minimum value is taken as corresponding to a loose TS$_2$, found to be placed at a zero energy barrier with respect to products CH$_3$Cl + Cl. It is depicted in
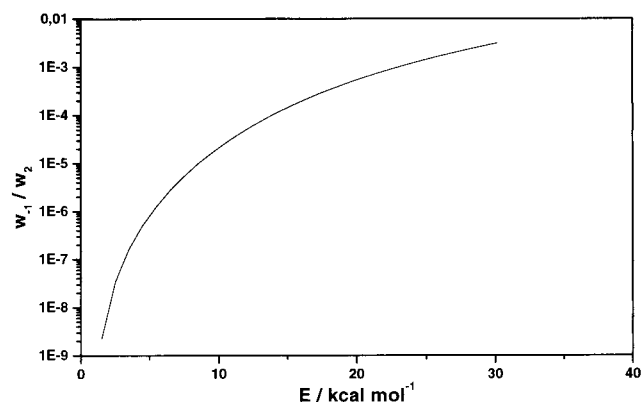
Figure 3. The ratio of the number of states, W_{-1}/W_2 vs accessible reaction energies E.

TABLE 4: Number of States for the Forward and Backward Elementary Steps of Reaction 3

E/ kcal mol^{-1}	W_2	W_{-1}
0.5	7.18E+11	0.00
1.5	9.59E+11	2.15E+03
3.5	1.67E+12	2.68E+05
6.5	3.67E+12	1.02E+07
10.5	9.70E+12	2.62E+08
17.5	4.46E+13	1.32E+10
25.5	2.06E+14	3.21E+11

Figure 1 and its properties along with all the required RRKM input that contains the moments of inertia and the harmonic frequencies of all the stationary points are summarized in Table 3. We may also notice here that the loose TS$_2$ is much lower located than TS$_1$, which implies $W_2 \gg W_{-1}$ for the important energy region. Thus, the term $W_2/(1 + \beta)$ in eq 5 reduces to a very good approximation to W_{-1}. This indicates that the tight transition state TS$_1$, at the entrance valley of the reaction, is the main important feature of the potential energy surface and the elaborate investigation of TS$_2$ is really insignificant. The fact is clearly demonstrated in Table 4 where a sample of W_{-1} and W_2 values vs E are collected and also in Figure 3 where the ratio W_{-1}/W_2 vs all accessible energies E is depicted. The diagram shows that W_{-1} remains much lower than W_2 for all the important energy region, making the first step in reaction 3 the rate-determining step for the CH$_3$ + Cl$_2$ system.

The rate constant is evaluated from eq 5 at 298 K. Since the temperature dependence of the macrocanonical rate coefficient is an important issue in the study of alkyl + dihalogen reactions, $k(T)$ calculations have been performed at two additional temperatures 450 and 600 K. Maximum J and E values used are 51 and 8 kcal mol^{-1}, respectively, at 300 K and 90 and 25 kcal mol^{-1} at 600 K with intermediate J and E values for 450 K. The theoretical results along with the experimental data are presented in Table 6 and they clearly indicate a definite increase in the rate constant with increasing T as a result of the sensitivity of the system to TS$_1$. In our opinion our theoretical results are in reasonable agreement with the experimental trends, taking into account the uncertainty associated with the ab initio calculations and the uncertainty in the experimental measurements.

4. Trajectory Calculations and Results

In addition to RRKM computations, quasiclassical trajectory (QCT) calculations were also carried out on a LEPS-type potential energy surface,[32] constructed to reproduce the lowest adiabatic PES of the system. The potential energy function of

TABLE 5: Properties of the Constructed LEPS Surface

species	r_e(Q−Cl)/ Å	r_e(Cl−Cl)/ Å	β(Q−Cl)/ Å^{-1}	ΔE^a/ kcal mol^{-1}	S^b
TS$_1$	3.050	2.101		0.95	
				1.24^c 2.40^c	
				0.51^d 0.53^d	
M$_2$	1.751	2.260		34.23	
				32.44^c 34.82^c	
QCl	1.779		1.723	88.24^e	0.551
Cl$_2$		1.999	2.008	58.03^e	0.042

^{a} With respect to reactants including ZPE corrections. ^{b} Sato parameters. ^{c} The ab initio results of present work and of ref 16, respectively. ^{d} The experimental estimates of refs 8 and 11, respectively. ^{e} The binding energies of these species.

TABLE 6: Calculated and Experimental Rate Constants in 10^{-12} cm^3 Molecule^{-1} s^{-1}

k (T)	RRKM	QCT	expt.^{a}	expt.^{b}	expt.^{c}
300 K	2.20	2.15	1.5(± 0.1)	2.0(± 0.4)	3.4(± 0.3)
450 K	2.48	2.62	2.41^d		
600	2.60	2.94	2.55^d		

^{a} Reference 12. ^{b} Reference 8. ^{c} Reference 11. ^{d} These experimental results correspond really to 437 and 579 K in ref 8.

London, Eyring, Polanyi, and Sato, despite its simplicity, has been widely used successfully for the kinetic and dynamic study of triatomic systems with a collinear or a near collinear saddle point geometry[33] and it can be easily used as the starting point for the construction of PES for more complex polyatomic systems.[34] The present system with a collinear C−Cl−Cl geometry in the transition state configuration TS$_1$ should be adequately described to a first approximation by a LEPS-type surface in which the CH$_3$ group is treated as a pseudoatom Q of mass equal to the total mass of CH$_3$.[35,36] A quite similar approach has been used in the quasi-classical trajectory study of the dynamics of the relevant CH$_3$ + I$_2$ system with good results.[37]

The surface, optimized to produce the best fitting to the ab initio results for the stationary points, takes into account the ZPE corrections and presents a potential energy well of 34.2 kcal mol^{-1} at C−Cl and Cl−Cl distances of 1.75 and 2.26 Å, respectively. It also presents a transition state corresponding to TS$_1$, located at 0.95 kcal mol^{-1} above reactants at a Cl−Cl distance 2.10 Å and a Q−Cl distance 3.05 Å. This distance is larger than the C−Cl distance of 2.27 Å of the CCSD(T) calculations for TS$_1$, and the corresponding value of Bozzelli et al.[16] but the difference is not expected to affect seriously the description of the reaction, since TS$_1$ is located anyway early enough in the entrance valley. The barrier height 0.95 kcal mol^{-1} of the calculated surface is quite low and is found in good consistency with the most recent experimental estimates.[11] The optimum Sato parameters along with the other molecular properties of the surface are summarized in Table 5 and a contour diagram for the collinear approach of reactants is given in Figure 4. Using Muckerman's quasi-classical trajectory program[39] we have calculated the reactive cross section, $\sigma_r(E_t)$, for a series of initial translational energy values, E_t, from 0.5 to 80.0 kcal mol^{-1}. A total of 30 000 trajectories were run at each value of E_t. Due to the large number of trajectories the calculated error[33] in each result is quite low. The initial conditions for Cl$_2$ were chosen to be the zero vibrational level and the rotational number $J = 20$ which is the most probable rotational level at 298 K. The reactive cross section is calculated
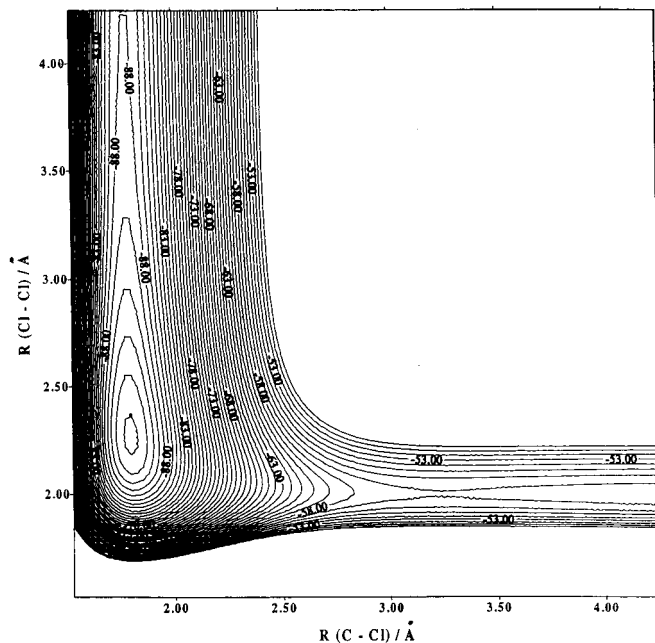
Reaction of Methyl Radicals with Chlorine Molecules

J. Phys. Chem. A, Vol. 106, No. 26, 2002 **6343**

Figure 4. The PES representation for the collinear approach C−Cl−Cl of the reactants. Energy values are in kcal mol^{-1} and the contour spacing corresponds to 1 kcal mol^{-1}.
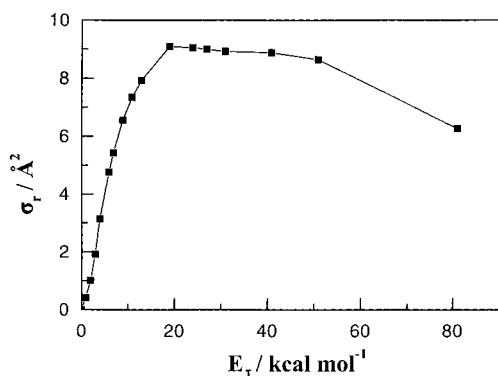

Figure 5. The variation of the reactive cross section vs initial collision energy.

from

$$\sigma(E_t) = \pi b_{max}^2 (E_t) [N_r(E_t)/N_{tot}(E_t)] \qquad (7)$$

where b_{max} is the calculated optimal maximum impact parameter at each E_t. The appropriate b_{max} values were found to increase with increasing collision energy and range from 4.0 to 4.5 Å for the range of energies examined in this study. $N_r(E_t)$ is the number of reactive trajectories and $N_{tot}(E_t)$ is the total number of trajectories run at a certain value of E_t. The reactive cross section is depicted as a function of the initial collision energy in Figure 5. As we can see the cross section increases considerably when increasing the initial translational energy of the reaction up to about 20 kcal mol^{-1}. This result is in reasonable agreement with the experimental studies of Kovalenko and Leone[12] who have found that the reaction rate is considerably enhanced for translationally "hot" methyl radicals. These workers have shown that the enhancement in reactivity observed is predominantly due to the translational excitation of CH$_3$. Thus, the dynamical behavior of the reaction appears to follow precisely the energy requirement rules[40] for reactions with an early barrier and shows an enhanced reactivity with the initial collision energy increase. Over 20 kcal mol^{-1} an
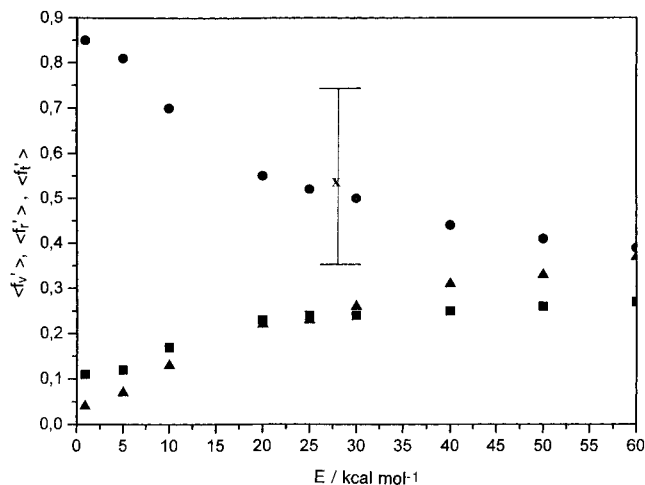

Figure 6. The variation of the fractions of total available energy disposed into product vibration $\langle f_v' \rangle$ (circles), rotation $\langle f_r' \rangle$ (triangles) and translation $\langle f_t' \rangle$ (squares). The experimental result by Kovalenko and Leone[12] is marked by an X and the error bars indicate the experimental uncertainty.

approximate plateau is obtained and further yet the rate coefficient begins to decline gradually for larger values of E_t. The rate coefficient at 298 K is calculated from

$$k(T) = g \left[\frac{8}{(k_B T)^3 \pi \mu} \right]^{1/2} \int_{E_0}^{\infty} E_t \sigma_r(E_T) \exp\left(\frac{-E_t}{k_B T} \right) dE_t \qquad (8)$$

where μ is the reactant reduced mass, E_0 is the threshold energy which is taken as 0.5 kcal mol^{-1} from Figure 5, and k_B is the Boltzmann contant. The rate constant at a given temperature is calculated by a polynomial fitting of the $\sigma_r(E_t)$ vs E_t curve. The multiple surface factor g is included to ensure counting reactive collisions only on the lowest adiabatic electronic PES of ($^2A_2''$)-CH$_3$ + ($^1\Sigma_g^+$)Cl$_2$ system. Since the intermediate M$_2$ formed is in a singlet state the g factor is taken as 1/2. The calculated rate coefficient is in turn included in Table 4 along with the RRKM results and the experimental values and a reasonable consistency is overall observed.

To examine the temperature dependence of the rate coefficient by the use of QCT technique, $k(T)$ has been calculated also at 450 and 600 K by repeating the above procedure and using as most probable rotational numbers for Cl$_2$, the values 25 and 28, respectively. The QCT results included in Table 6, reflect adequately the experimental trends. They show some greater tendency to increase with increasing temperature as a result of the lower barrier, 0.95 kcal mol^{-1}, of the best fitted surface compared to 1.24 kcal mol^{-1} of the ab initio calculations. This point indicates further the sensitivity of the system to the low energy barrier at the entrance of the reaction.

The simplicity of the LEPS functional form allows us readily to study the mode of disposal of the total available energy to compare with the experimental results. The total available energy, E_{tot}, results from the difference in binding energies between reactants and products, ΔD_e, the collision kinetic energy, E_t, and the internal energy of the reactants, which includes the considerable zero-point energy of CH$_3$. This energy is distributed among product translational and internal energies, i.e.,

$$E_{tot} = \Delta D_e + E_t + E_{int} = E_t' + E_{int}' \qquad (9)$$

where the primes indicate product quantities. Figure 6 shows the variation of the average fractions of product vibration,
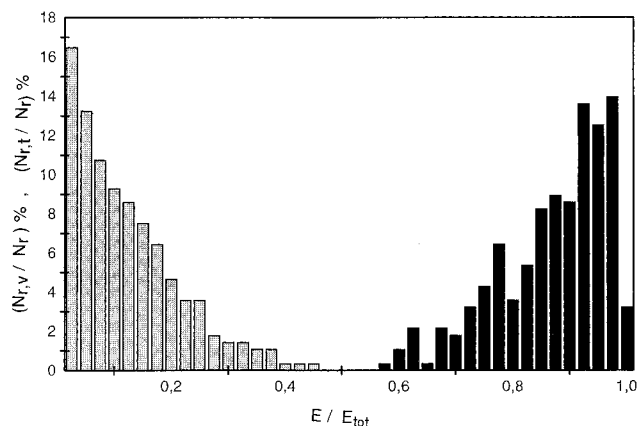
Figure 7. The distribution of product translation (left histogram) and vibration (right histogram) at 0.85 kcal mol^{-1}. $(N_{r,t}/N_r)$ % or $(N_{r,v}/N_r)$ % indicates the percentage of reactive encounters possessing a certain amount of product energy into translation or vibration.
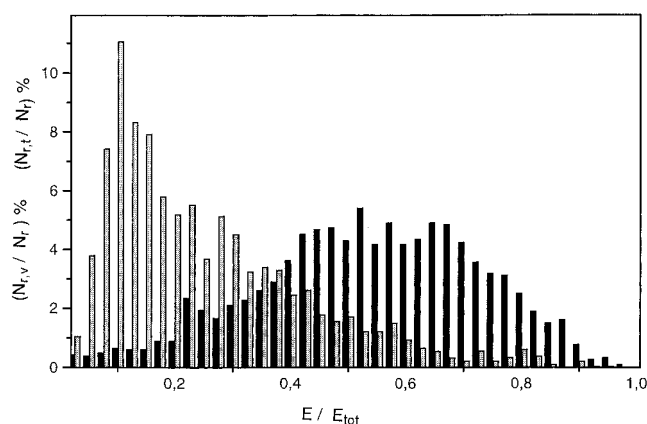

Figure 8. The same as in Figure 7 at 25 kcal mol^{-1}.

rotation, and translation, $\langle f_v{}' \rangle$, $\langle f_r{}' \rangle$ and $\langle f_t{}' \rangle$ as functions of the energy of the system. At very low energies all of the available energy goes into product vibration. As the energy rises, $\langle f_v{}' \rangle$ decreases slowly reaching 0.4 at 60 kcal mol^{-1}. The experimental result of Kovalenko and Leone[12] taking into account the large experimental uncertainty, fits reasonably well within the theoretical curve as shown in Figure 5.

The detailed distribution of total available energy into product vibration and translation at $E_t = 0.85$ and 25.0 kcal mol^{-1}, is depicted in Figures 7 and 8, respectively. In these diagrams we plot the percentage of the total reactive encounters $N_{r,v}/N_r$ or $N_{r,t}/N_r$, possessing a specific fraction of product energy into either vibration or translation, respectively, vs the energy of the system. $N_{r,v}$ or $N_{r,t}$ represents the number of reactive collisions with a certain amount of vibrational or translational energy and N_r is the total number of reactive trajectories at given collision energy E_t. We clearly see that at $E_t = 0.85$ kcal mol^{-1} the major part of the total reactive encounters leads to products with high vibrational excitation and low translational energy and thus, the considerable exothermicity of the reaction at $E_t = 0.85$ kcal mol^{-1} is directed almost exclusively into product vibration. At $E_t = 25.0$ kcal mol^{-1} this fraction decreases although the products still show a large part of total energy directed into vibration. Hence we may conclude that the theoretical treatment describes reasonably well the observed reaction dynamics indicating that the reaction is favored in near-collinear collisions of methyl radicals with Cl$_2$ on a PES with an early energy barrier. The CH$_3$Cl molecules produced are vibrationally excited since a considerable amount of the reaction

exoergicity is deposited preferably into product vibration. This behavior is found to be quite analogous to the dynamics observed in the CH$_3$ + I$_2$ system[37,40] where an optimal activation energy barrier of 0.8 kcal mol^{-1} has been employed to simulate the kinetics of the system.[37]

Summary

Quantum mechanical calculations for the CH$_3$ + Cl$_2$ reaction have been carried out to determine the stationary points along the reaction path. The system passes through a shallow minimum M$_1$ to a tight transition state TS$_1$ located at an energy barrier 1.24 kcal mol^{-1} with respect to reactants at the CCSD(T)// MP2-(full)/ 6-311+G(3df, 3dp) level of theory. It further proceeds to a deep minimum M$_2$ at 32.44 kcal mol^{-1} which decomposes into CH$_3$Cl + Cl. Extended RRKM calculations and quasi-classical trajectory computations based on the ab initio results describe satisfactorily the kinetics and dynamics of the reaction observed experimentally and in particular the small but definitely positive temperature dependence, resulting from the sensitivity of the system to TS$_1$. The main conclusions of the study are the considerable enhancement in reactivity obtained with increasing the initial collision energy, and the favored disposal of total available energy into product vibration, in reasonable agreement with the experimental observations.

References and Notes

(1) Mark, H. F.; Othmer, D. F.; Overberger, C. G.; Seaborg, G. T., Eds.; *Encyclopedia of Chemical Technology*, 3rd ed.; Wiley: New York, 1979; Vol. 5.
(2) Molina, M. J.; Rowland, F. S. *Nature* (London) **1974**, *249*, 810.
(3) Levine, R. D.; Bernstein, R. B. *Molecular Reaction Dynamics and Chemical Reactivity*; Oxford: New York, 1987.
(4) Seakins, P. W.; Pilling, M. J.; Niranen, J. T.; Gutman, D.; Krasnaperow, L. N. *J. Phys. Chem.* **1992**, *96*, 9847.
(5) Timonen, R. S.; Seetula, J. A.; Gutman, D. *J. Phys. Chem.* **1990**, *94*, 3005.
(6) Evans, B. S.; Whittle, E. *Int. J. Chem. Kinet.* **1978**, *10*, 745.
(7) McFadden, D. L.; McCullough, E. A.; Kalos, F.; Ross, J. *J. Chem. Phys.* **1973**, *59*, 121.
(8) Timonen, R. S.; Gutman, D. *J. Phys. Chem.* **1986**, *90*, 2987.
(9) Timonen, R.; Kalliorine, K.; Koskikallio, F. *Acta Chem. Scand. A* **1986**, *40*, 459.
(10) Timonen, R. *Ann. Acad. Sci. Fenn., Ser. A2* **1988**, *218*, 5.
(11) Dobis, O.; Benson, S. W. *Zeis. Physik. Chem.* **2001**, *215*, 283.
(12) Kovalenko, L. J.; Leone, S. *J. Chem. Phys.* **1984**, *80*, 3656.
(13) Benson, S. W.; Dobis, O. *J. Phys. Chem. A* **1988**, *102*, 5175.
(14) Tirtowidjojo, M. M.; Colegrove, B. T.; Durant, J. L., Jr. *Ind. Eng. Chem. Res.* **1995**, *34*, 4202.
(15) Seetula, J. A. *J. Chem. Soc., Faraday Trans.* **1998**, *94*, 3561.
(16) Lee, I.; Bozzelli, J. W.; Sawerysyn, J. P. *Int. J. Chem. Kinet.* **2000**, *32*, 548.
(17) Gonzalez, C.; Schlegel, H. B. *J. Phys. Chem.* **1989**, *90*, 2154.
(18) Frisch, M. J.; Trucks, G. W.; Schlegel, H. B.; Scuseria, G. E.; Robb, M. A.; Cheeseman, J. R.; Zakrzewski, V. G.; Montgomery, J. A., Jr.; Stratmann, R. E.; Burant, J. C.; Dapprich, S.; Millam, J. M.; Daniels, A. D.; Kudin, K. N.; Strain, M. C.; Farkas, O.; Tomasi, J.; Barone, V.; Cossi, M.; Cammi, R.; Mennucci, B.; Pomelli, C.; Adamo, C.; Clifford, S.; Ochterski, J.; Petersson, G. A.; Ayala, P. Y.; Cui, Q.; Morokuma, K.; Malick, D. K.; Rabuck, A. D.; Raghavachari, K.; Foresman, J. B.; Cioslowski, J.; Ortiz, J. V.; Stefanov, B. B.; Liu, G.; Liashenko, A.; Piskorz, P.; Komaromi, I.; Gomperts, R.; Martin, R. L.; Fox, D. J.; Keith, T.; Al-Laham, M. A.; Peng, C. Y.; Nanayakkara, A.; Gonzalez, C.; Challacombe, M.; Gill, P. M. W.; Johnson, B. G.; Chen, W.; Wong, M. W.; Andres, J. L.; Head-Gordon, M.; Replogle, E. S.; Pople, J. A. *Gaussian 98*, revision A.1; Gaussian, Inc.: Pittsburgh, PA, 1998.
(19) Gonzàlez, M.; Hijazo, J.; Novoa, J. J.; Sayos, R. *J. Chem. Phys.* **1998**, *108*, 3168.
(20) Joseph, T.; Steckler, R.; Truhlar, D. G. *J. Chem. Phys.* **1987**, *87*, 7036.
(21) Kurosaki, Y.; Takayanagi, T. *Chem. Phys. Lett.* **1999**, *299*, 57.

Reaction of Methyl Radicals with Chlorine Molecules

J. Phys. Chem. A, Vol. 106, No. 26, 2002 **6345**

(22) Hoffmann, M. A.; Smith, D. J.; Bradshaw, N.; Grice, R. *Mol. Phys.* **1986**, *57*, 1219.

(23) Mozurkewich, M.; Benson, S. W. *J. Phys. Chem.* **1984**, *88*, 6429.

(24) Chen, Y.; Rauk, A.; Tschuikow-Roux, E. *J. Phys. Chem.* **1991**, *95*, 9900.

(25) Simonson, M.; Bradley, K. S.; Schatz, G. C. *Chem. Phys. Lett.* **1995**, *244*.

(26) Steinfeld, J. I.; Francisco, J. S.; Hase, W. L. *Chemical Kinetics and Dynamics*; Prentice Hall: New Jersey, 1989.

(27) Baer, T.; Hase, W. L. *Unimolecular Reaction Dynamics*; Oxford: New York, 1996.

(28) Zhu, L.; Hase, W. L. QCPE-644.

(29) Liu, Y.-P.; Lu, D.-H.; Gonzalez-Lafont, A.; Truhlar, D. G.; Garrett, B. C. *J. Am. Chem. Soc.* **1993**, *115*, 7806.

(30) Guadagnini, R.; Schatz, G. C.; Walch, S. P. *J. Phys. Chem. A* **1998**, *102* 5857.

(31) Drougas, E.; Papayannis, D. K.; Kosmas, A. M. *Chem. Phys.,* in press.

(32) Eyring, H.; Henderson, D.; Jost, W. *Physical Chemistry, an Advanced Treatise*, v. VIA; Academic: New York, 1974.

(33) Baer, M. *Theory of Chemical Reaction Dynamics*, v. III; CRC Press: Boca Raton, FL, 1985.

(34) Espinosa-Garc'ia, J. *J. Phys. Chem. A* **2001**, *105*, 134.

(35) Nyman, G.; Clary, D. C. *J. Chem. Phys.* **1994**, *101*, 5756.

(36) Nyman, G.; Clary, D. C.; Levine, R. D. *Chem. Phys.* **1995**, *191*, 223.

(37) Ree, J.; Kim, Y. H.; Shin, H. K. *Chem. Phys. Lett.* **1997**, *272*, 419.

(38) Muckerman, J. T. QCPE-229.

(39) Polanyi, J. C.; Wong, W. H. *J. Chem. Phys.* **1969**, *51*, 1439.

(40) Hunter, T. F.; Kristjansson, K. S. *J. Chem. Soc., Faraday Trans. 2* **1982**, 2067.